Case Report

A rare inherited homozygous missense variant in *PLA2G6* influences susceptibility to infantile neuroaxonal dystrophy: a case report

Yongxue Lyu[1], Tao Wang[2]^, Meifang Lin[1], Fengfeng Qi[1]

[1]Department of Pediatric Health Care, Huzhou Maternity & Child Health Care Hospital, Huzhou, China; [2]Key Laboratory of Digital Technology in Medical Diagnostics of Zhejiang Province, Dian Diagnostics Group Co., Ltd., Hangzhou, China

Contributions: (I) Conception and design: F Qi; (II) Administrative support: F Qi; (III) Provision of study materials or patients: Y Lyu; (IV) Collection and assembly of data: Y Lyu, T Wang, M Lin; (V) Data analysis and interpretation: Y Lyu, T Wang, M Lin; (VI) Manuscript writing: All authors; (VII) Final approval of manuscript: All authors.

Correspondence to: Fengfeng Qi, BM. Department of Pediatric Health Care, Huzhou Maternity & Child Health Care Hospital, No. 2 East Street, Huzhou 313000, China. Email: qiff2006@163.com.

Background: Infantile neuroaxonal dystrophy (INAD) is an ultra-rare early-onset autosomal recessive neurodegenerative disorder due to *PLA2G6* variants. The clinical symptoms of INAD patients display considerable diversity, and many *PLA2G6* variants are still not thoroughly investigated in relation to their associated clinical presentations.

Case Description: A 16-month-old boy was admitted to our hospital due to regression of acquired motor and speech abilities that had persisted for 4 months. The patient was born to a healthy consanguineous couple after 41 weeks of pregnancy and natural delivery. Before 12 months old, he had normal motor development milestones. On admission, he also showed astasia-abasia, weakness of distal muscles, and diminished patellar tendon reflex. Brain magnetic resonance imaging (MRI) revealed cerebellar atrophy. Auditory brainstem response (ABR) indicated moderately severe hearing loss. With chromosome microarray analysis (CMA), we identified several copy number-neutral regions of runs of homozygosity (ROH) in the patient. Whole-exome sequencing (WES) further revealed that the patient harbored a homozygous missense variant NM_003560.2: c.1778C>T, p.Pro593Leu (rs1451486649) in the *PLA2G6* gene. In the patient's asymptomatic parents and brother, the *PLA2G6* c.1778C>T variant stayed in heterozygous status as confirmed by Sanger sequencing. The patient was finally diagnosed with INAD.

Conclusions: We report an INAD child with a rare *PLA2G6* c.1778C>T homozygous missense variant and associated clinical symptoms. The family-based cosegregation analysis reveals that the *PLA2G6* c.1778C>T homozygous variant contributes to the pathogenesis of INAD.

Keywords: Infantile neuroaxonal dystrophy (INAD); *PLA2G6*; c.1778C>T; neuropathological disorders; case report

Submitted Nov 28, 2023. Accepted for publication Feb 01, 2024. Published online Mar 20, 2024.
doi: 10.21037/tp-23-568
View this article at: https://dx.doi.org/10.21037/tp-23-568

^ ORCID: 0000-0002-2952-134X.

Introduction

Infantile neuroaxonal dystrophy (INAD; OMIM # 256600), originally named Seitelberger's disease, is an ultra-rare early-onset neurological disorder with an autosomal recessive manner of inheritance (1-3). INAD's prevalence is unknown, but its clinical manifestations have slowly been recognized from the cases described so far. Infants with typical INAD usually experience a short asymptomatic period after birth (4). Most of them, from the age of 6 months or even earlier, consistently develop multiple neuropathological symptoms, including but not limited to progressive psychomotor deterioration, mental retardation, axial hypotonia, cerebellar ataxia, hearing loss (HL), and optic nerve abnormalities, that jointly lead to a persistent vegetative state and premature death, generally early in the first decade of life (4,5). There is growing evidence that INAD is primarily caused by various loss-of-function variants in the phospholipase A2 group VI (*PLA2G6*) gene on chromosome 22q, while genetic and phenotypic heterogeneity exists (6-10). Nowadays, the definitive diagnosis of INAD heavily relies on genetic confirmation of *PLA2G6* status in combination with the INAD clinical phenotypes. To date, in the Human Gene Mutation Database (HGMD), more than 100 *PLA2G6* variants, the vast majority of which are missense variants, have been associated with INAD (7). However, the association between an individual's genetic makeup (genotype) and the clinical characteristics (phenotype), i.e., genotype-phenotype association, is still lacking for many INAD patients attributed to *PLA2G6* variants.

Here, we report a 16-month-old boy with typical clinical symptoms of INAD. Chromosomal microarray analysis (CMA) detected several copy number-neutral regions of runs of homozygosity (ROH), which involve dozens of recessively inherited diseases related genes, including the *PLA2G6* gene. By whole-exome sequencing (WES), we identified a rare homozygous missense variant in the exon 13 of *PLA2G6*, i.e., NM_003560.2: c.1778C>T, p.Pro593Leu (rs1451486649), which was further checked in the proband's family by Sanger sequencing analysis. As a result, we found that asymptomatic members in the enrolled family were all heterozygous carriers of the *PLA2G6* c.1778C>T variant. Our study emphasizes that genetic testing is essential for the early and accurate identification of INAD and reveals that *PLA2G6* c.1778C>T homozygous variant contributes to the pathogenesis of INAD. We present this article in accordance with the CARE reporting checklist (available at https://tp.amegroups.com/article/view/10.21037/tp-23-568/rc).

Highlight box

Key findings

- We report an infantile neuroaxonal dystrophy (INAD) child with a rare *PLA2G6* c.1778C>T homozygous missense variant and associated clinical symptoms.

What is known and what is new?

- INAD is an ultra-rare early-onset neurological disorder caused by *PLA2G6* variants. However, genotype-phenotype association is still lacking for a majority of *PLA2G6* variants.
- We enrolled a 16-month-old boy with classical INAD neuropathological symptoms and his family members. By chromosome microarray analysis, whole-exome sequencing, and Sanger sequencing, we identified a *PLA2G6* c.1778C>T homozygous missense variant in the child. By family-based cosegregation analysis, we confirmed that the *PLA2G6* c.1778C>T homozygous variant contributes to the pathogenesis of INAD.

What is the implication, and what should change now?

- Our study emphasizes that genetic testing is essential for the early and accurate identification of INAD and reveals that *PLA2G6* c.1778C>T homozygous variant contributes to the pathogenesis of INAD.

Case presentation

Clinical manifestation

A 16-month-old boy (*Figure 1A*; II-3) was admitted to our hospital due to regression of acquired motor and speech abilities that had persisted for four months. The proband was born to a healthy consanguineous couple (*Figure 1A*; I-1, 30 years old; I-2, 30 years old) after 41 weeks of pregnancy and natural delivery. He had two brothers: the oldest brother (*Figure 1A*; II-1, 5 years old) died of respiratory failure caused by muscle dysfunction, and the other brother (*Figure 1A*; II-2, 5 years old) was healthy. At birth, the proband's weight was 3.6 kg and height was 50 cm, and no obvious physical defects were noticed by his parents. He displayed head rotation and neck extension from 3 months of age; started rolling over at 4 months old; learned to sit up independently and walk with assistance at 7 and 11 months old, respectively. The first simple words "dada" and "mama" started at 12 months old. At that time, he was able to ask for something by pointing. Later on, the proband

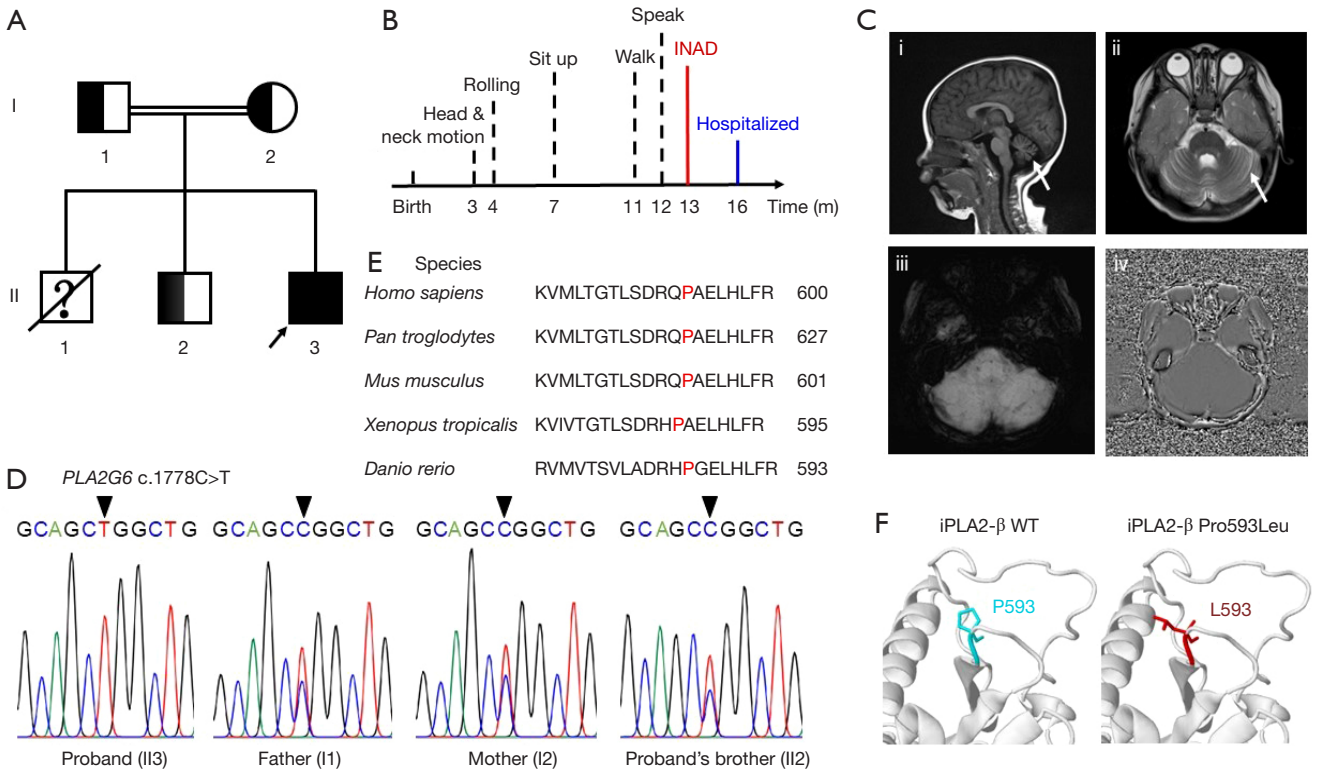

Figure 1 Clinical and genetic analysis of the investigated family. (A) The pedigree of the investigated family. The arrow indicates the proband. *PLA2G6* c.1778C>T heterozygous variant carriers are marked with semisolid color. The question mark indicates that genotype is not investigated. The diagonal line indicates that person is deceased. (B) The timeline of the proband's main motor development events before hospitalization. (C) Brain MRI of the proband. The sagittal T2-weighted image (i) and axial T2-weighted FLAIR image (ii) show widened bilateral cerebral hemispheres and cerebellar sulci. The white arrow in (i) and (ii) indicates cerebellar atrophy and bright cerebellar cortex, respectively. The axial SWI images (iii, iv) show the absence of brain iron accumulation. (D) Sanger sequencing of *PLA2G6* c.1778C>T. The results show the proband with a homozygous *PLA2G6* c.1778C>T variant and the proband's parents and elder brother with the same heterozygous mutation; the black arrow indicates the identified variant position. (E) Sequencing alignment of iPLA2-β among five species using the NCBI COBALT (RRID:SCR_004152). Proline 593 of iPLA2-β was highlighted in red. (F) Zoom-in iPLA2-β WT structure (left) and iPLA2-β P593L (right). The proteins were structured by the Missense3D online software (11). m, months; INAD, infantile neuroaxonal dystrophy; WT, wide type; MRI, magnetic resonance imaging; FLAIR, fluid-attenuated inversion recovery; SWI, susceptibility weighted imaging; NCBI, national center for biotechnology information.

gradually lost his speech ability and showed lessened and stereotypic body movements. At the time of physical and neurological examination, he had a weight of 11 kg and a height of 82 cm. Notably, he failed to sit up by himself and developed astasia-abasia but could respond to "no" and simple instructions. The motor development timeline is summarized in *Figure 1B*. The electroencephalogram (EEG) showed normal activity. However, weakness of distal muscles and diminished patellar tendon reflex, but not pathologic reflexes, were observed. Brain magnetic resonance imaging (MRI) showed bilateral widening of the cerebellar sulci, indicating cerebellar atrophy, but brain iron accumulation was absent (*Figure 1C*). The auditory brainstem response (ABR) indicated moderately severe HL. His left ear had 60 decibels (dB) HL and the right ear had 70 dB HL. Moreover, the serum biochemical analysis showed a noticeable reduction in creatinine (19.7 μmol/L) and elevated levels of several enzymes, including aspartate aminotransferase (AST; 68 U/L), lactate dehydrogenase (LDH; 365.7 U/L), alkaline phosphatase (ALP; 135.6 U/L), and creatine kinase-myoglobin binding (CK-MB; 36.3 IU/L), and rest important indexes were within normal laboratory ranges (Table S1). Due to these clinical and laboratory findings, the

Table 1 Gene mutations detected in the proband by WES analysis

Gene	Reference sequence	Variant	Protein consequence	Alleles status	VEP annotation	Interpretation in ClinVar	Inherited pattern	Related disease (s)
PLA2G6	NM_003560.2	c.1778C>T	p.Pro593Leu	Homozygous	Missense	Likely pathogenic, uncertain significance	AR	Infantile neuroaxonal dystrophy 1
								Neurodegeneration with brain iron accumulation 2B
								Parkinson disease 14
TRIP12	NM_004238.1	c.592T>G	p.Ser198Ala	Heterozygous	Missense	Not reported	AD	Clark-Baraitser syndrome
TBR1	NM_006593.2	c.1351_1356dup	p.Ala451_Gly452dup	Heterozygous	Frameshift	Not reported	AD	Intellectual developmental disorder with autism and speech delay
ASXL3	NM_030632.1	c.2065A>C	p.Ile689Leu	Heterozygous	Missense	Benign	AD	Bainbridge-Ropers syndrome
VPS53	NM_001128159.3	c.1517G>A	p.Arg506Gln	Heterozygous	Missense	Uncertain significance	AR	Pontocerebellar hypoplasia, type 2E
HSD17B4	NM_000414.3	c.508G>A	p.Gly170Ser	Heterozygous	Missense	Not reported	AR	Perrault syndrome 1
								D-bifunctional protein deficiency
PDE10A	NM_001130690.2	c.62G>C	p.Ser21Thr	Heterozygous	Missense	Not reported	AR	Dyskinesia, limb and orofacial, infantile onset
							AD	Striatal degeneration
ATP13A2	NM_022089.2	c.1447T>G	p.Tyr483Asp	Heterozygous	Missense	Not reported	AR	Spastic paraplegia 78
								Kufor-Rakeb syndrome

WES, whole-exome sequencing; VEP, variant effect predictor; AR, autosomal recessive; AD, autosomal dominant.

proband was highly suspected with INAD, and this family was enrolled for further genetic analysis.

Genetic analysis

For the etiology screening of rare neurodevelopment disorders, especially for individuals born to consanguineous parents, chromosome microarray analysis (CMA) is the priority selection. Since CMA offers the capacity to detect ROH regions, in addition to copy number variants (CNVs) and single nucleotide polymorphisms (SNPs), for all chromosomes. Importantly, extensively existing ROH regions contain low-penetrance genes that are usually associated with recessively inherited diseases and increase susceptibility to them. Therefore, we performed CMA (Appendix 1), which revealed approximately 69 Mb ROH regions across the proband's genome, but not CNVs. The ROH regions (>10 Mb) includes 1p21.3-p12 (19.09 Mb; 23 genes; 98,957,502–118,049,185 GRCh37), 4q31.21-q32.1 (14.41 Mb; 12 genes; 143,073,691–157,490,504 GRCh37), and 22q12.2-q13.31 (16.05 Mb; 21 genes; 31,245,745–47,297,593 GRCh37). Notably, *PLA2G6* gene is located within the ROH region of 22q12.2-q13.31 (Table S2).

To make an accurate genetic diagnosis, we further implemented WES followed by Sanger sequencing in the investigated family (Appendix 1). After filtering out the common and non-coding variants, WES analysis found that the only homozygous variant that may reasonably explain INAD-like symptoms of the proband was NM_003560.2: c.1778C>T, p.Pro593Leu (rs1451486649) homozygous missense variant in *PLA2G6* gene, while in several INAD-irrelevant genes, variants were all present in the heterozygous state (*Table 1*). Sanger sequencing confirmed the *PLA2G6* homozygous variant in the proband and further revealed that the proband's parents and alive sibling were all heterozygous for *PLA2G6* c.1778C>T (*Figure 1D*). The identified rare *PLA2G6* c.1778C>T was previously known as a likely pathologic variant with ClinVar star 2^+ according to the American College of Medical Genetics and

Genomics (ACMG) guidelines. *PLA2G6* c.1778C>T has a total allele frequency of 3×10^{-6} in GnomAD, but it was not included in ExAC (Exome Aggregation Consortium), 1000 Genomes Project, HapMap, and our homemade exome database.

Molecular analysis

Conservation analysis of *PLA2G6*-encoded protein, iPLA2-β, indicated that Pro593 is a highly conserved site from Danio rerio to Homo sapiens (*Figure 1E*). *PLA2G6* c.1778C>T homozygous variant results in the replacement of the hydrophobic and cyclic amino acid proline (Pro593) located in the iPLA2-β catalytic domain (CAT) by another hydrophobic, but aliphatic, amino acid leucine (Pro593Leu) (*Figure 1F*). This missense variant is predicted to be pathogenic by functional analysis with SIFT (RRID:SCR_012813) (12), PolyPhen2 (RRID:SCR_013189) (13), and ClinPred (14). Thus, the proband was diagnosed with INAD, which was potentially caused by a rare inherited *PLA2G6* c.1778C>T homozygous pathologic variant.

Ethical considerations

All procedures performed in this study were in accordance with the ethical standards of the Ethics Committee of the Huzhou Maternity & Child Health Care Hospital and with the Helsinki Declaration (as revised in 2013). Written informed consent was obtained from the patient's legal guardians for the publication of this case report and accompanying images. A copy of the written consent is available for review by the editorial office of this journal.

Discussion

The *PLA2G6* gene, which encodes a Ca^{2+}-independent phospholipase A2 (iPLA2-β), is located on chromosome 22q13.1 and contains 19 exons, including two alternative exons (15). *PLA2G6* is a well-known pathogenic gene for a series of autosomal recessively inherited neurodegenerative diseases, mainly including INAD, atypical neuroaxonal dystrophy (AND), and early-onset parkinsonism (AREP) (7). Collectively, the term *PLA2G6*-associated neurodegeneration (PLAN) has been derived to describe all diseases resulting from *PLA2G6* gene variants (7). Among PLAN, INAD is recognized by the earliest onset of psychomotor deterioration and the shortest life span (7). This phenomenon is likely attributed to the fact that INAD-related *PLA2G6* variants result in more severe impairment of iPLA2-β enzymatic activity compared to *PLA2G6* variants linked to other PLAN disorders (16). It is also noteworthy that the same *PLA2G6* variant can lead to different clinical phenotypes among individuals (8,9,17,18). For example, compared to our INAD proband, patient (43-year-old man) with the *PLA2G6* c.991G>T homozygous variant, which causes a 70% reduction in enzyme activity of iPLA2-β, developed AREP phenotypes with relatively later onset ages and slower disease progression (17). However, his younger sister (34 years old) with the same homozygous variant displayed no symptoms of PLAN (17).

In this study, our INAD proband carried *PLA2G6* c.1778C>T homozygous variant, which causes a conserved proline substitution by leucine in the iPLA2-β CAT. The mammalian iPLA2-β harbors two CATs, which are widely recognized for their dual roles in regulating iPLA2-β enzymatic activity (19). On one hand, CATs harbor active sites directly engaged in the phospholipid hydrolysis reaction (19). On the other hand, they also contribute to the iPLA2-β dimerization process (19). Given that leucine lacks the cyclic structure found in proline, the Pro593Leu substitution has the potential to introduce conformational change(s) in CATs and impact iPLA2-β dimerization. In addition, leucine is aliphatic and typically more soluble in water than proline, which may influence the hydrophobicity of CATs and impact molecular interactions with active sites. Maybe due to aforementioned factors, predictive tools like SIFT, PolyPhen2, and ClinPred have all indicated that *PLA2G6* c.1778C>T variant to be deleterious. ClinVar database has included *PLA2G6* c.1778C>T variant and defines it as a likely pathologic variant. Actually, in 2016, Al-Maawali *et al.* first reported the co-occurrence of *PLA2G6* c.1778C>T variant and *PLA2G6* c.1974C>A variant in an INAD patient (20). Nevertheless, limited clinical information of this patient was described (20). From this solely available report, one can hardly make an accurate assessment of the contribution of *PLA2G6* c.1778C>T to the pathogenesis of INAD. In this study, we detected the *PLA2G6* c.1778C>T homozygous variant in a 16-month-old boy and described his INAD clinical characterization in detail. His inbred parents and alive sibling were all asymptomatic and, importantly, heterozygous for *PLA2G6* c.1778C>T. These results clearly suggest that the proband's *PLA2G6* c.1778C>T homozygous variant is recessively inherited from both parents and leads to INAD.

Before the discovery of the linkage between *PLA2G6*

variants and INAD pathogenesis in 2006 (2,3), the diagnosis of INAD mainly relied on a spectrum of unspecific clinical phenotypes. However, the most initial noticeable INAD symptoms, i.e., psychomotor regression and muscle weakness may also lead to a diagnosis of other neurodevelopment disorders, such as hereditary spastic paraplegia (HSP) (21). In most patients, brain MRI detects cerebellar atrophy early in INAD. As INAD progresses, on T2-weighted MRI, gradient echo (GRE), or susceptibility-weighted imaging (SWI), abnormal low signals commonly appear primarily in the globus pallidus, indicating iron accumulation. However, cerebellar atrophy and iron accumulation also can be found in several other diseases (6). Besides, iron accumulation appears only at the late stage of INAD (4,5). In the patient with *PLA2G6* c.1778C>T/c.1974C>A compound heterozygous variants, brain iron accumulation was absent at age of 2 years (20). In consistent with this, we also failed to detect iron accumulation in our patient at the age of 16 months. Thus, MRI provides limited benefit for early INAD diagnosis. Notably, in *PLA2G6*-mutant patients, the observation of elevated AST and LDH levels (22,23), which were confirmed in our proband, raises the possibility that these two enzymes represent potential biomarkers of INAD. Our findings also indicated reduced creatinine levels and elevated ALP/CK-MB levels in the proband, indicating a widespread enzyme metabolism disorder and, possibly, kidney, heart, and multiple tissue damage. Furthermore, axon spheroids and vacuoles revealed by peripheral nerve biopsies have long been regarded as a gold standard for INAD diagnosis, with an estimated 87% of *PLA2G6* mutation-positive INAD having axon spheroids (5). However, parents of INAD children have a less than enthusiastic response to cooperating with peripheral nerve biopsies, once they are informed of its invasive procedures, at least in our case.

To date, treatments of INAD and other PLAN are still palliative. Enzyme replacement therapy and gene therapy, as innovative approaches to rectify iPLA2-β enzyme activity, are still in the early stages of development (1). In our case, the proband's parents decided to refrain from any treatment because of the similar disease experience of their first child. We provided the couple with counseling on in vitro fertilization (IVF), preimplantation genetic diagnosis (PGD), and prenatal diagnosis if they wanted to have another child.

It is crucial to highlight that the proband harbored four heterozygous variants in pathogenic genes associated with autosomal dominant (AD) diseases (*Table 1*). While *ASXL3* c.2065A>C (NM_030632.1; rs563644271) is classified as a benign variant in ClinVar, the interpretations of the remaining variants have not been documented. Notably, heterozygous variants in the *TRIP12*, *TBR1*, and *PDE10*A are known to cause Clark-Baraitser syndrome (CLABARS; OMIM # 617752), intellectual development with autism and speech delay (IDDAS; OMIM # 606053), and autosomal-dominant striatal degeneration (ADSD; OMIM # 616922), respectively (24-26). All the three rare diseases show neurological symptoms or signs. In general, CLABARS is characterized by intellectual disability, developmental delay, macrocephaly, and distinct facial deformities (24). Autism spectrum disorder and delayed speech and intellectual functions are hallmark signs of IDDAS (25). Clinical symptoms of ADSD include slowly progressive dysarthria, gait disturbance, muscle rigidity, and dysdiadochokinesia (26). At clinical level, progressive neurological regression and the absence of physical deformities stand out as the distinguishing features of INAD when compared to CLABARS and IDDAS. Muscle weakness and hypotonia are distinctive features that set apart INAD from ADSD in affected patients. Meanwhile, onset and age of presentation are also helpful for differential diagnosis. Even though the enrolled family did not exhibit the classic symptoms of CLABARS, IDDAS, and ADSD, we cannot dismiss the possibility that *TRIP12*, *TBR1*, and *PDE10*A variants are *de novo*, which may predispose the proband to those AD diseases in the future.

We acknowledge several limitations of the present study. First, we did not perform peripheral nerve biopsies to examine axon spheroids. Second, we cannot exclude the possibility that multiple heterozygous variants (*Table 1*) may also contribute to the proband's symptoms. Furthermore, the tracking time of the proband was short, making clinical characterization of INAD progression difficult. From the latest telephone follow-up, we were informed that the proband only made tiny movements in bed at the age of 2.5 years. Ultimately, more research is required to determine the mechanism by which the *PLA2G6* c.1778C>T homozygous variant alters the activity of iPLA2-β and leads to INAD.

Conclusions

In summary, we reported detailed clinical characteristics of an INAD patient bearing *PLA2G6* c.1778C>T homozygous variant. Our study expands the genetic and clinical spectrum of *PLA2G6* pathogenic variants and provides important

information about the pathogenesis of *PLA2G6*-related INAD.

Acknowledgments

We are grateful to the patient and his family, as well as the help of all the physicians in the course of the medical care.
Funding: This work was supported by grants from Huzhou Science and Technology Project of Zhejiang Province (No. 2022GYB54 to Y.L.).

Footnote

Reporting Checklist: The authors have completed the CARE reporting checklist. Available at https://tp.amegroups.com/article/view/10.21037/tp-23-568/rc

Peer Review File: Available at https://tp.amegroups.com/article/view/10.21037/tp-23-568/prf

Conflicts of Interest: All authors have completed the ICMJE uniform disclosure form (available at https://tp.amegroups.com/article/view/10.21037/tp-23-568/coif). Y.L. receives funding from Huzhou Science and Technology Project of Zhejiang Province (Funding No. 2022GYB54). T.W. is a current employee of Dian Diagnostics Group Co., Ltd., Hangzhou, Zhejiang Province. The other authors have no conflicts of interest to declare.

Ethical Statement: The authors are accountable for all aspects of the work in ensuring that questions related to the accuracy or integrity of any part of the work are appropriately investigated and resolved. All procedures performed in this study were in accordance with the ethical standards of the Ethics Committee of the Huzhou Maternity & Child Health Care Hospital and with the Helsinki Declaration (as revised in 2013). Written informed consent was obtained from the patient's legal guardians for the publication of this case report and accompanying images. A copy of the written consent is available for review by the editorial office of this journal.

References

1. Babin PL, Rao SNR, Chacko A, et al. Infantile Neuroaxonal Dystrophy: Diagnosis and Possible Treatments. Front Genet 2018;9:597.
2. Morgan NV, Westaway SK, Morton JE, et al. PLA2G6, encoding a phospholipase A2, is mutated in neurodegenerative disorders with high brain iron. Nat Genet 2006;38:752-4. Erratum in: Nat Genet 2006;38:957.
3. Khateeb S, Flusser H, Ofir R, et al. PLA2G6 mutation underlies infantile neuroaxonal dystrophy. Am J Hum Genet 2006;79:942-8.
4. Altuame FD, Foskett G, Atwal PS, et al. The natural history of infantile neuroaxonal dystrophy. Orphanet J Rare Dis 2020;15:109.
5. Deng X, Yuan L, Jankovic J, et al. The role of the PLA2G6 gene in neurodegenerative diseases. Ageing Res Rev 2023;89:101957.
6. Gregory A, Kurian MA, Maher ER, et al. PLA2G6-Associated Neurodegeneration. In: Adam MP, Feldman J, Mirzaa GM, et al. editors. GeneReviews®. Seattle, WA, USA: University of Washington, Seattle, 2008.
7. Guo YP, Tang BS, Guo JF. PLA2G6-Associated Neurodegeneration (PLAN): Review of Clinical Phenotypes and Genotypes. Front Neurol 2018;9:1100.
8. Rostampour D, Zolfaghari MR, Gholami M. Novel insertion mutation in the PLA2G6 gene in an Iranian family with infantile neuroaxonal dystrophy. J Clin Lab Anal 2022;36:e24253.
9. Ansari B, Nasiri J, Namazi H, et al. Infantile Neuroaxonal Dystrophy in Two Cases: Siblings with Different Presentations. Iran J Child Neurol 2022;16:193-8.
10. Zou Y, Luo H, Yuan H, et al. Identification of a Novel Nonsense Mutation in PLA2G6 and Prenatal Diagnosis in a Chinese Family With Infantile Neuroaxonal Dystrophy. Front Neurol 2022;13:904027.
11. Khanna T, Hanna G, Sternberg MJE, et al. Missense3D-DB web catalogue: an atom-based analysis and repository of 4M human protein-coding genetic variants. Hum Genet 2021;140:805-12.
12. Ng PC, Henikoff S. SIFT: Predicting amino acid changes that affect protein function. Nucleic Acids Res 2003;31:3812-4.
13. Adzhubei I, Jordan DM, Sunyaev SR. Predicting functional

effect of human missense mutations using PolyPhen-2. Curr Protoc Hum Genet 2013;Chapter 7:Unit7.20.
14. Alirezaie N, Kernohan KD, Hartley T, et al. ClinPred: Prediction Tool to Identify Disease-Relevant Nonsynonymous Single-Nucleotide Variants. Am J Hum Genet 2018;103:474-83.
15. Larsson Forsell PK, Kennedy BP, Claesson HE. The human calcium-independent phospholipase A2 gene multiple enzymes with distinct properties from a single gene. Eur J Biochem 1999;262:575-85.
16. Engel LA, Jing Z, O'Brien DE, et al. Catalytic function of PLA2G6 is impaired by mutations associated with infantile neuroaxonal dystrophy but not dystonia-parkinsonism. PLoS One 2010;5:e12897.
17. Shi CH, Tang BS, Wang L, et al. PLA2G6 gene mutation in autosomal recessive early-onset parkinsonism in a Chinese cohort. Neurology 2011;77:75-81.
18. Chu YT, Lin HY, Chen PL, et al. Genotype-phenotype correlations of adult-onset PLA2G6-associated Neurodegeneration: case series and literature review. BMC Neurol 2020;20:101.
19. Malley KR, Koroleva O, Miller I, et al. The structure of iPLA(2)β reveals dimeric active sites and suggests mechanisms of regulation and localization. Nat Commun 2018;9:765.
20. Al-Maawali A, Yoon G, Feigenbaum AS, et al. Validation of the finding of hypertrophy of the clava in infantile neuroaxonal dystrophy/PLA2G6 by biometric analysis. Neuroradiology 2016;58:1035-42.
21. Murala S, Nagarajan E, Bollu PC. Hereditary spastic paraplegia. Neurol Sci 2021;42:883-94.
22. Dastsooz H, Nemati H, Fard MAF, et al. Novel mutations in PANK2 and PLA2G6 genes in patients with neurodegenerative disorders: two case reports. BMC Med Genet 2017;18:87.
23. Kraoua I, Romani M, Tonduti D, et al. Elevated aspartate aminotransferase and lactate dehydrogenase levels are a constant finding in PLA2G6-associated neurodegeneration. Eur J Neurol 2016;23:e24-5.
24. Aerden M, Denommé-Pichon AS, Bonneau D, et al. The neurodevelopmental and facial phenotype in individuals with a TRIP12 variant. Eur J Hum Genet 2023;31:461-8.
25. McDermott JH, Study DDD, Clayton-Smith J, et al. The TBR1-related autistic-spectrum-disorder phenotype and its clinical spectrum. Eur J Med Genet 2018;61:253-6.
26. Mencacci NE, Kamsteeg EJ, Nakashima K, et al. De Novo Mutations in PDE10A Cause Childhood-Onset Chorea with Bilateral Striatal Lesions. Am J Hum Genet 2016;98:763-71.

Cite this article as: Lyu Y, Wang T, Lin M, Qi F. A rare inherited homozygous missense variant in *PLA2G6* influences susceptibility to infantile neuroaxonal dystrophy: a case report. Transl Pediatr 2024;13(3):484-491. doi: 10.21037/tp-23-568

Supplementary

Table S1 Main results of the proband's serum biochemical examination

Items	Value	Reference range
Enzymes		
ALT (U/L)	20	9.0–50.0
AST (U/L)	68	15.0–45.0
AST/ALT ratio	3.4	0.23–2.47
ALP (U/L)	135.6	45.0–125.0
GGT (U/L)	11.3	10.0–60.0
LDH (U/L)	365.7	100.0–240.0
CK (U/L)	85	24.0–194.0
CK-MB (IU/L)	36.3	0.0–25.0
Metabolism		
Bilirubin, total (μmol/L)	4.4	2.0–22.0
Bilirubin, direct (μmol/L)	0.8	0.0–6.0
Bilirubin, indirect (μmol/L)	3.6	0.0–16.0
Serum proteins		
Protein, total (g/L)	77.1	65.0–85.0
Hemoglobin (g/L)	118	110–160
Albumin (g/L)	48.8	40.0–55.0
Globulin (g/L)	28.3	20.0–40.0
A/G ratio	1.72	1.2–2.4
Serum electrolytes		
Cl^- (mmol/L)	102	96–108
Ca^{2+} (mmol/L)	1.28	1.05–1.29
Na^+ (mmol/L)	143	135–145
K^+ (mmol/L)	4.26	3.5–5.5
HCO_3^- (mmol/L)	22.8	22.0–27.0
Kidney function		
BUN (mmol/L)	4.31	2.86–8.20
Creatinine (μmol/L)	19.7	49.0–97.0
Uric acid (μmol/L)	135.1	149.0–416.0
Thyroid function		
TSH (μIU/mL)	1.93	0.35–5.5
Triiodothyronine (nmol/L)	3.25	0.89–2.44
Thyroxine (nmol/L)	135.5	62.68–150.84

ALT, alanine aminotransferase; AST, aspartate aminotransferase; ALP, alkaline phosphatase; GGT, gamma-glutamyl transferase; LDH, lactate dehydrogenase; CK, creatine kinase; CK-MB, creatine kinase-myoglobin binding; A/G, albumin/globulin; BUN, blood urea nitrogen; TSH, thyroid-stimulating hormone.

https://dx.doi.org/10.21037/tp-23-568

Table S2 ROH regions detected by CMA

ROH regions	Size (kb)	Genes	Inherited pattern
4q31.21-q32.1	14417	*SLC10A7*	AR
		FGA	AR
		FGB	AR
		FGG	AR
		TRIM2	AR
		LRBA	AR
		LRAT	AR
		GAB1	AR
		MMAA	AR
		MAB21L2	AD/AR
		TDO2	AR
		GUCY1A3	AR
1p21.3-p12	19092	*AGL*	AR
		AMPD1	AR
		IGSF3	AR
		PTPN22	AD/AR
		AMPD2	AR
		SLC35A3	AR
		TSHB	AR
		CDC14A	AR
		NGF	AR
		GPR88	AR
		SARS	AR
		COL11A1	AR
		CASQ2	AR
		LRIG2	AR
		RNPC3	AR
		SLC16A1	AD/AR
		GPSM2	AR
		ALX3	AR
		AP4B1	AR
		DBT	AR
		TAF13	AR
		SASS6	AR
		DRAM2	AR
22q12.2-q13.31	16052	*LARGE1*	AR
		XPNPEP3	AR
		NCF4	AR
		CYP2D6	AR
		TRIOBP	AR
		TXN2	AR
		NDUFA6	AR
		SLC5A1	AR
		CSF2RB	AR
		TRMU	AR
		DNAL4	AR
		ACO2	AR
		MCM5	AR
		FBXO7	AR
		PLA2G6	AR
		NAGA	AR
		TMPRSS6	AR
		CYB5R3	AR
		IFT27	AR
		TNFRSF13C	AR
		ADSL	AR

ROH, runs of homozygosity; CMA, chromosome microarray analysis; AR, autosomal recessive; AD, autosomal dominant.

https://dx.doi.org/10.21037/tp-23-568

Appendix 1

DNA extraction

Peripheral blood was collected from the members of the enrolled family. Total genomic DNA was isolated by using QIAamp® DNA Blood Mini Kit (Qiagen GmbH, Germany) according to the manufacturer's protocol. DNA purity and concentration were further measured by a NanoDrop spectrophotometer.

Chromosome microarray analysis (SNP-array)

Detection of genomic CNVs was performed with AffymetrixCytoScan HD (Affymetrix, Santa Clara, USA) following the manufacturer's instructions. Array results were visualized and analyzed by Chromosome Analysis Suite software (Affymetrix GeneChip Convert Console, Santa Clara, USA) and Chromosome Analysis Suite Version 2.0.0. Log2 ratio and B allele frequency (BAF) values were plotted along chromosomal coordinates, allowing the detection of both copy number changes and copy neutral ROH. The size threshold for CNVs analysis was set at >50 kb for gains, >25 kb for losses, and >10 Mb for loss of heterozygosity. Data interpretation followed the ACMG guideline.

Whole exome sequencing

For whole-exome sequencing of the proband, 1~3 μg genomic DNA was used for fragmentation, and DNA library construction was prepared according to the manufacturer's protocols (Agilent Technologies, Inc., Santa Clara, CA, USA). Genomic DNA was randomly fragmented to an average size of 150–220 bp by Covaris® S220 sonicator (Thermofisher, MA, USA). DNA fragments were end-repaired and phosphorylated, followed by A-tailing and ligation at the 3' ends with paired-end multiple indexing adaptors. The quality of the DNA library was assessed using Life Qubit Fluorometer 3.0 and Agilent 2200 TapeStation Instrument (Agilent Technologies, Inc.). Sequencing was performed on the Illumina HiSeq X-ten (Illumina, CA, USA) in high-output mode with 150 bp paired-end reads. The original sequencing data were analyzed by FastQC software. Reads were aligned to the human reference sequence (GRCh37/hg19) using the Burrows-Wheeler Aligner tool (v0.7.15-r1140). The Genome Analysis Toolkit tool (v3.7-0) was used for base quality-score recalibration, calling, and filtering variants. Data were annotated with the Annovar and VEP software. Data interpretation followed the ACMG guideline.

Sanger sequencing

The *PLA2G6* c.1778C>T variant was confirmed by Sanger sequencing. Primers that were designed by Primer3 software according to information on the mutation site. Forward primer, ccacctatcccgaacagagg. Reverse primer, ctggtggaaggcaggtacag. Amplification of primers was performed using polymerase chain reaction (PCR), then screened by Mutation Surveyor. The genomic DNA samples of the enrolled family were analyzed by Sanger sequencing to determine variant status.

https://dx.doi.org/10.21037/tp-23-568